Transferability of Results of PTS Experiments to the Integrity Assessment of Reactor Pressure Vessels

E. Roos, U. Eisele, L. Stumpfrock

MPA Stuttgart, Pfaffenwaldring 32, 70569 Stuttgart, Germany

IAEA Specialists' Meeting, Esztergom, Hungary, May 5 - 8, 1997

Abstract

The integrity assessment of the reactor pressure vessel (RPV) is based on the fracture mechanics concept as provided in the code. However, this concept covers only the linear-elastic fracture mechanics regime on the basis of the reference temperature RT_{NDT} as derived from charpy impact and drop-weight test.

The conservatism of this concept was demonstrated for a variety of different materials covering optimized and lower bound material states with regard to unirradiated and irradiated conditions.

For the elastic-plastic regime, methodologies have been developed to describe ductile crack initiation and stable crack growth. The transferability of both, the linear-elastic and elastic-plastic fracture mechanics concept was investigated with the help of large scale specimens focusing on complex loading situations as they result from postulated thermal shock events for the RPV.

A series of pressurized thermal shock (PTS) experiments were performed in which the applicability of the fracture mechanics parameters derived from small scale specimen testing could be demonstrated. This includes brittle (static and dynamic) crack initiation and crack arrest in the low charpy energy regime as well as stable crack initiation, stable crack growth and crack arrest in the upper shelf toughness regime. The paper provides the basic material data, the load paths, representative for large complex components as well as experimental and theoretical results of PTS experiments. From these data it can be concluded that the available fracture mechanics concepts can be used to describe the component behavior under transient loading conditions.

1 Introduction

In Germany the procedure for the integrity assessment of the reactor pressure vessel (RPV), the material requirements and the loading conditions to be regarded are fixed e.g. in KTA [1].

In the safety assessment of the RPV the incredibility for initiation of a brittle fracture has to be demonstrated throughout the entire life-time for all service loading conditions including postulated accidents. Basis for the safety analysis is a semi-elliptical flaw in the cylindrical shell of the RPV. Since this assumption is most challenging, the fracture mechanics understanding of material behaviour and the necessary concepts and tools will be discussed in this paper with respect to PTS application . Besides sufficient material ductility which has to be proved by Charpy-V-notch impact tests, the analysis may be based on fracture

toughness on the basis of the fracture mechanics concept of the Code or on fracture mechanics parameters experimentally determined with material of the component.

2 Technical aim

According to the Code [1,2] the exclusion of brittle fracture has to be assured for the reactor pressure vessel of a nuclear power plant under all service and accident conditions. For the analysis a crack has to be postulated that is perpendicular to the maximum principle stress. For conditions A and B acc. to KTA the postulated flaw is assumed to be a surface flaw with a depth of 0.25 x wall thickness and an effective length of 1.5 x wall thickness. For conditions C and D the flaw dimension to be assumed is twice the size that can be detected by advanced non destructive examination.

The loading of the crack is characterised by the stress intensity factor K_I. Failure by brittle fracture is avoided if K_I is lower than the corresponding material parameter K_{Ic}. The appropriate material parameter can be selected from the K_{Ic} curve. In case that crack initiation cannot be excluded, crack arrest has to be proved before the crack penetrates 75 % of the wall thickness. For characterising crack arrest a large number of linear-elastically determined dynamic fracture mechanics data (K_{Id}) and crack arrest data (K_{Ia}) were evaluated and presented in [3] that lead to the K_{Ia} curve which is the basis of the reference curve K_{IR} of the ASME and the KTA Code. The tests were performed with materials typical for nuclear application. The individual material properties are implemented by normalising the fracture toughness data to the nil ductility transition temperature T_{NDT} as recommended by Pellini 1969 [4] and an early edition of [2]. In later editions of the ASME Code and in the KTA Code the reference temperature RT_{NDT} was chosen as normalising temperature instead of T_{NDT}. The assessment of safety against brittle failure in case of flaws detected in service is performed in a similar way, considering first the case of crack initiation.

3 Fracture Mechanics Parameters

The procedure of determining fracture mechanics parameters experimentally is described in detail in the common Standards. There exist Standards according to the material behaviour for the linear-elastic and for the elastic-plastic regime as well.

3.1 Linear-Elastic Fracture Mechanics Parameters

The linear-elastic fracture mechanics parameter is the fracture toughness K_{Ic}. The K_{Ic} value is characteristic for the initiation of a brittle fracture. The procedure to determine K_{Ic} values is given in the U.S. Test Standard ASTM E 399 [5], in the British Standard BS 5447 [6] and in the ISO/DSI Draft 12 737 [7]. All three Standards are essentially identical. The Standards contain criteria to assure linear-elastic behaviour up to fracture and to meet the requirements for plane-strain conditions. The K_{Ic} values determined by that procedure are supposed to be size independent.

3.2 Elastic-Plastic Fracture Mechanics Parameters

In the region of elastic-plastic material behaviour the crack tip opening displacement (CTOD) and the J-Integral can be used as fracture mechanics parameter, as well. With these parameters it is possible to determine the crack resistance of a material experimentally. Plotting the J-Integral vs the amount of stable crack extension leads to the "crack resistance curve" of the material. From the crack resistance curve crack initiation values can be derived according to the following Standards and drafts:

- ASTM E 813 (J_{Ic}) [8]
- European Structural Integrity Society: ESIS P1/P2 (J_i, $J_{0,2}$, $J_{0,2/bl}$) [9]
- Deutscher Verband für Materialprüfung: DVM ($J_{0,2/bl}$, J_i) [10]

At MPA Stuttgart, since several years a procedure is applied additionally to the procedures mentioned above that is based on J_i values derived from the crack resistance curve and the

"stretched zone" [11 - 15], since the crack resistance curve (J_R-curve) itself is not a material law. This procedure has been implemented also in the European recommendation ESIS P2 for the determination of fracture mechanics parameters.

As shown in [13, 14, 15] the J_{Ic}, $J_{0.15}$, $J_{0.2}$ and $J_{0.2/bl}$ values may be used as technological parameters which are suitable for a qualitative comparison of different materials. For characterising the physical process of crack initiation, however, only the effective crack initiation value can be used since this parameter is independent of specimen size and geometry and is not influenced by the stress state in the structure.

The crack initiation value J_i [14] is based on the determination of the "stretched zone" Δa_i. This is the region at the crack tip of large plastic deformation ("blunting") before the event of stable crack extension. The physical background of this procedure is the fact that after the process of blunting, the stretched zone has reached its final size which is sustained during the complete process of stable crack growth. Tests with specimens of different amount of stable crack extension confirmed this assumption [16, 17]. After the test, the stretched zone can be determined in a perpendicular projection of the crack plane with the help of a scanning electron microscope.

For the quantitative determination of the crack initiation value J_i, that point of the J_R-curve (J-Δa-curve) is selected for which Δa equals Δa_i. To obtain a reliable J_i value high performance of the measuring technique is required so that sufficient reliable data are provided in the region of small Δa values that have to be fitted by an adequate polynomium. The dense covering of the J_R-curve with data pairs in the region of small Δa values is the main feature of the procedure developed at MPA Stuttgart in comparison with other procedures. Fig 1 shows the variety of different initiation values as they were determined by various procedures. It can clearly be seen that only J_i is not effected by significant amount of stable crack growth.

3.3 Crack arrest toughness

The procedure to determine crack arrest toughness values for ferritic materials is described in ASTM E 1221 [18]. The crack is initiated under a given amount of energy and while the crack propagates, the stress intensity decreases. The K_{Ia}-value is the stress intensity at the crack tip after the crack has arrested. It is a substitute parameter but represents a lower limit that covers the dynamic crack arrest parameter K_{IA} conservatively [19]. To obtain valid K_{Ia}-values linear-elastic material behaviour and plane strain conditions are required as for static crack initiation values.

The unstable crack extension which is the required starting point to achieve crack arrest data is realised by initiating the crack in a high strength (brittle) weld bead. The determination of crack arrest data in the elastic-plastic regime is limited by the ductility of the material. Usually K_{Ia} values cannot be determined at temperatures $T > T_{NDT} + 60$ K because sufficient unstable crack extension before arrest cannot be assured by applying present test procedures.

4 Transferability of Fracture Mechanics Concepts and Material Parameters to Components

The transferability of fracture mechanics concepts and material parameters is verified when data derived form small scale specimen testing can describe the material behaviour of large complex structures and stress states. This means in particular that the concepts must reliably enable a prediction of crack initiation, regardless if brittle or ductile failure occurs, on the basis of K_{Ic} or J_i-values, respectively, and in the elastic-plastic regime the prediction of the amount of stable crack growth based on the J-integral.

4.1 Transferability to Mechanically Loaded Structures

In the frame of the research programme FKS crack resistance curves were determined on large scale specimens [12, 13]. The crack initiation values were determined according to the procedure applied at small scale specimens as described in chapter 3.

The K_{IJ}-values derived from J_i of specimens with different size and geometry (CT specimens with thickness $B \geq 100$ mm, single edge (SECT), double edge (DECT) and center cracked (CCT) tension specimens as well as three point bend (TPB) specimens with $100 \text{ mm} \leq B \leq 600$ mm and $2W = 200$ mm) are plotted together with the scatter band of initiation values obtained for small scale specimens. For the three materials with different upper shelf Charpy energy (170, 90 and 40 J) it shows that the effective crack initiation value J_i is not depending on specimen size and geometry. This proves that J_i and the corresponding K_{IJ}-value can be applied to all structures, fig. 2.

The general application of fracture mechanics parameters, however, is limited to the initation value J_i. The crack resistance curves itself does not represent an universal material law but is characteristic for an individual specimen or component [20, 21,22]. Fig. 3 shows crack resistance curves determined with the modified 22 NiMoCr 3 7 base material and specimens of different geometry and size.

It has to be assumed that specimens with little stable crack extension incorporate a distinct three dimensional stress state with the consequence of limited possibility for plastic deformation. Under extreme conditions, plastic deformation may be suppressed completely so that initiation is immediately followed by brittle fracture.

For the quantification of the three dimensional stress state in the ligament of a structure the coefficient of multiaxiality $q = \frac{\tau_r}{\sigma_m}$ can be used [21, 23]. In this equation τ_r is the reduced stress acc. to Hencky and σ_m the mean stress.

Using the invariants, q can be expressed in the form of

$$q = \left(\frac{-9 J_2'}{J_1^2} \right)^{1/2}$$

with J'_2 as the second invariant of the deviator and J_1 as the first invariant of the stress tensor. From a mechanistic point of view q describes the interaction of slip mechanisms characterised by J'_2 and fission mechanisms characterised by J_1. The highest degree of mulitaxiality occurs in case of the hydrostatic stress state and leads to the value of $q = 0$.

The quantification of the stable crack growth is also possible by analysing the coefficient of multiaxiality across the ligament of a specimen or a component.

4.2 Transferability Thermally Transient Loaded Structures

The transferability of fracture mechanics concepts and material parameters to structures which are subjected to thermally transient load, was proved at MPA Stuttgart by means of thick walled hollow cylinders under thermal shock loading [24, 25, 26]. The results were compared with the predictions according to the Code.

The basic component and material behaviour will be demonstrated with the help of three experiments referred to as NKS 4-1, NKS 6 and NT3 out of a series of 8 experiments. Two specimens contained a circumferential crack the third one two partial circumferential cracks. Geometric and material parameters of the specimens are given in table 1, (see also fig. 4).

Specimen	NKS 4-1	NKS 6 compound specimen	NT 3
material	22 NiMoCr 3 7 "modified"	MoV steel "special heat"	MoV steel „special heat"
Charpy upper shelf energy			
- base material (b.m.)	60 J	30 J	70 J
- weld metal	-	220 J	-
yield strength (b.m.)	506 MPa	1092 MPa	692 MPa
ultimate strength (b.m.)	789 MPa	1165 MPa	824 MPa
T_{ref} (not corresp. to RT_{NDT})	120°C	250°C	140°C
inner radius R_i			
- base material	200 mm	202 mm	200 mm
- weld metal	-	296 mm	-
outer radius R_a	400 mm	402.5 mm	395 mm
crack length	2 x 52°	360°	360°C
crack depth	31.2 / 59.5 mm	34 mm	20 mm
a_o/W	0.15	0.17	0.10
crack growth	1.5 / 0.9 mm	61 mm	48.5 mm

Table 1: Geometry and material of selected PTS specimens

Two materials have a Charpy energy of less than 68 J, therefore, the reference temperature RT_{NDT} could not be determined acc. to the Code. Even the nil ductility transition temperature could not be determined for all materials since at the necessary high temperatures unstable crack initiation could not be realised. For this reason a transition temperature was derived from the instrumented Charpy impact test taking crack arrest load P 4 = 4 kN and portion of ductile fracture FATT 50 into account. The transition temperature was selected as the lower temperatures from both of the above mentioned criteria and referred to as T_{ref}.

The result of the NKS 4-1 experiment is plotted in fig 5 and shows the stress intensity factor K_I - calculated for the deepest point of the crack on the basis of the J-Integral - for this transient loading on the one hand and on the other hand the initiation values K_{IJ} derived from J_i of the material vs temperature.

The load path intersects the crack initiation curve at high temperature in the ductile regime which leads to stable crack initiation. Since the stress intensity factor further increases with decreasing temperature, stable crack growth occurs up to the point when the maximum in the load path is reached. After that point no further crack growth was detected not even when the K_{Ic}-curve of the material was intersected. This can be explained firstly by the fact that the K_{Ic}-curve does not represent the mean material behaviour but obviously an upper bound, secondly that the K_{Ic}-curve is limited in the K-axis by the material specific curve for ductile crack initiation derived form J_i and thirdly that the load path already starts to decrease while intersecting the K_{Ic}-curve which excludes crack initiation in principle.

Nevertheless of the low Charpy upper shelf energy of 60 J at 200°C crack initiation occurred in a ductile mode and the process can be described by the J-Integral. The stable crack growth at the deepest point amounts for both cracks to 1.5 and 0.9 mm, respectively. The crack did not extend in circumferential direction.

To assess the amount of stable crack growth the J_R-curves for temperature in the range of 200 to 280°C, fig 6, right part, are compared with the load path, fig 6, left part. For the J_{max}-value of the load path an amount of stable crack growth of 1.5 mm can be determined from the J_R-curve. This good agreement with the value obtained form the experiment can be referred to the agreement in stress state which is essentially the same in both the CT specimens used for determination of the J_R-curves and the thermal shock specimen NKS 4-1, fig 7.

Different from the test specimen NKS 4-1 the specimen NKS 6 contained a circumferential crack. The compound specimen was composed of the MoV steel with low USE at the inner part and a weld metal (S 3 NiMo 1) with high USE at the outer part applied by the shape welding technique. After plating, the specimen was post weld heat treated for 10 hrs at 590°C.

The linear-elastic and elastic-plastic fracture toughness data are plotted in fig 8 and compared with the K_{Ic}-curve of the Code, however, normalised to T_{ref} and not to RT_{NDT}. The K_{Ic}-data are enveloped by the K_{Ic}-curve and the upper part of the K_{Ic}-curve is cut by the K_{IJ}-values in the ductile regime.

The load path K_I for the specimen NKS6 during the cooling phase is shown in fig 9 together with the fracture toughness curves K_{Ic} and K_{IR} (normalised to T_{ref} = 250°C of the base material) and the K_{IJ}-data of the weld metal. The first crack initiation occurred predominantly in a ductile mode which is in accordance with the experimentally established K_{IJ}-curve and at the first intersection of the load path with this curve. Subsequent a spontaneous crack jump of 20 mm occured. The crack was then arrested in the base material with low toughness. The fracture surface of this crack jump shows 100 % fission fracture. After further cooling a second crack initiation occurred. In this case both the region of crack initiation and the region where the crack extended showed ductile appearance. This second crack jump of 41 mm ended at the interface between base material and high tough weld metal. Accoustic emission signals showed clearly the spontaneous event of the first crack growth and signals over a period of time indicating ductile crack growth. The initiation values of the ductile weld metal which are also shown in fig 9, are much higher than those of the base material. Therefore conditions were given for crack arrest in the upper shelf. According to the load path a further ductile crack initiation with little crack growth might have occurred. It was not observed, however, probably because of the material scatter and the reduced driving force in the range of the maximum of the load path. The experiment shows that also for the NKS 6 test the initiation and arrest behaviour could be described. Initiation occurred in the range of the K_{Ic}-curve normalised to T_{ref} and this confirms essentially the fracture mechanics concept of the Code. Crack arrest occurred at lower temperature as predicted from the K_{Ic}-curve, e.g. the K_{Ia}-curve describes the arrest behaviour conservatively.

The load path K_I for the specimen NT3 during the cooling phase is shown in fig.10. The first initiation of the crack occurred when reaching the scatterband of small scale initiation values. The crack was arrested after some unstable crack growth due to decreasing crack tip loading and increasing temperature. After further cooling crack growth and subsequent crack arrest took place again in 8 events. After passing the maximum of the load path no further crack growth occurred. The crack path predicted with analytical methods is shown in fig. 11 in the critical crack depth diagramme. Based on experimentally determined initiation and arrest values a greater crack growth of (a_{max}/W = 0.57) is predicted than reached in the experiment (a_{max}/W = 0.35). Based on the fracture toughness curves of the code a crack growth of a_{max}/W = 0.81 would be predicted. So these curves describe the behaviour of the specimen NT3 conservatively.

The experiment NT3 showed 9 crack initiation - crack arrest events, which may be clearly seen by means of acoustic emission measurements. Each event had strong signals in a short time interval during crack propagation, fig. 12.

5 Summary

The safety analysis of a reactor pressure vessel (RPV) is based on the fracture mechanics concept which is implemented in the Code. The present Code, however, covers only the linear-elastic regime. The individual properties of a material are described by the reference temperature that results form Charpy impact and drop-weight test. The conservatism of this concept was proved for a variety of different materials which represent optimised quality as well as materials at the bounds of the specification (lower bound) and specification exceeding materials (worst case).

For the elastic-plastic regime methods were developed, in the past, to describe stable crack initiation and crack growth quantitatively on the basis of the J-Integral. The nuclear Codes have not yet adapted these concepts. With the help of large specimen tests, particularly considering complex loading situations, the transferability of both the linear-elastic and the elastic-plastic concepts could be confirmed.

A series of thermal shock experiments was performed to demonstrate the applicability of fracture mechanics parameters derived form small scale specimens to large structures with complex stress states. The experiments were aimed at static crack initiation and crack arrest in the low shelf region of Charpy impact energy on the one hand and on the other hand to crack initiation and stable crack growth in the Charpy upper shelf energy region. The thermal shock experiments were performed with large scale model structures with a wall thickness realistic with regard to the conditions of the cylindrical shell of a RPV. Crack initiation and crack growth could be described analytically. These experiments demonstrated the applicability of fracture mechanics concepts and material parameters to describe failure behaviour of large structures under transient conditions.

6 References

/1/ Sicherheitstechnische Regeln des Kerntechnischen Ausschusses (KTA). Komponenten des Primärkreises von Leichtwasserreaktoren. KTA 3201.2, Fassung 3/84

/2/ ASME Boiler and Pressure Vessel Code, Section III, Division 1, 1986

/3/ PVRC Recommendations on Toughness Requirements for Ferritic Materials, PVRC Ad Hoc Group on Toughness Requirements. WRC Bulletin 175, Aug. 1972

/4/ Pellini, W. S.: Evolution of Engineering Principles for Fracture-Safe Design of Steel Structures. NRL-Report 6957, 1969

/5/ ASTM E 399: Standard Test Method for Plane-Strain Fracture Toughness of Metallic Materials. Annual Book of ASTM Standards, Vol. 03.01.1990

/6/ BS 5447: Method of Plane Strain Fracture Toughness Testing. British Standards Institution, 1977

/7/ Metallic Materials - Determination of plane-strain fracture toughness. Draft International Standard ISO / DIS 12737, ISO 1993

/8/ ASTM E 813-88D: Standard Test Method for J_{Ic}, a Measure of Fracture Toughness. Annual Book of ASTM Standards, Vol. 03.01.1988

/9/ Prüfvorschlag der European Structural Integrity Society ESIS P1/P2 (1992), Procedure for Determining the Fracture Behaviour of Materials.

/10/ Ermittlung von Rißinitiierungswerten und Rißwiderstandskurven bei Anwendung des J-Integrals. DVM Merkblatt 002, Deutscher Verband für Materialprüfung e.V., Juni 1987

/11/ Roos, E.: Erweiterte experimentelle und theoretische Untersuchungen zur Quantifizierung des Zähbruchverhaltens am Beispiel des Werkstoffes 20 MnMoNi 5 5. Dissertation, Universität Stuttgart, 1982

/12/ Roos, E., U. Eisele, H. Silcher und D. Kiessling: Ermittlung von Rißwiderstandskurven auf der Basis des J-Integrals an Großproben. 13. MPA-Seminar, MPA Stuttgart, 8. - 9. Oktober 1987

/13/ Roos, E. and U. Eisele: Determination of Material Characteristic Values in Elastic Plastic Fracture Mechanics by Means of J-Integral Crack Resistance Curves. Journal of Testing and Evaluation, JTEVA, Vol. 16, No. 1, Jan. 1988, pp. 1-11

/14/ Roos, E.: Grundlagen und notwendige Voraussetzungen zur Anwendung der Rißwiderstandskurve in der Sicherheitsanalyse angerissener Bauteile. Fortschritt-Berichte VDI, Reihe 18, Nr. 122, 1993

/15/ Eisele, U. und E. Roos: Bestimmung bruchmechanischer Initiierungskenngrößen auf der Basis des J-Integrals. Materialprüfung 31, 1989, Vol. 10, pp. 323-327

/16/ Ohji, K., A. Otsuka and H. Kobayashi: Evaluation of Several J_{Ic} Testing Procedures Recommended in Japan. Elastic-Plastic-Fracture: Second Symposium, Volume II-Fracture Resistance Curves and Engineering Applications. ASTM STP 803, C. F. Shih and J. P. Gudas, Eds., American Society for Testing and Materials, 1983, pp. II-420 - II-438

/17/ Kobayashi, H., H. Nakamura and H. Nakazawa: Evaluation of Blunting Line and Elastic-Plastic Fracture Toughness. In Elastic-Plastic-Fracture: Second Symposium, Volume II-Fracture Resistance Curves and Engineering Applications. ASTM STP 803, C. F. Shih and J. P. Gudas, Eds., American Society for Testing and Materials, 1983, pp. II-420 - II-438

/18/ ASTM E 1221-88: Standard Test Method for Determining Plane-Strain Crack-Arrest Fracture Toughness, K_{Ia}, of Ferritic Steels. Annual Book of ASTM Standards, Vol. 03.01.1988

/19/ Roos, E., H. Beyer, T. Demler, R. Gillot, W. Imhof und A. Klenk: Werkstoffmechanische Untersuchungen, Teil A: Untersuchungen an Kleinproben. Abschlußbericht für Forschungsvorhaben Komponentensicherheit (FKS); Phase II, MPA Stuttgart, Oktober 1989

/20/ Roos, E., H. Silcher und U. Eisele: Zur Frage der "unteren Rißwiderstandskurve" als Werkstoffgesetz für eine bruchmechanische Bauteilbewertung. 15. MPA-Seminar, MPA Stuttgart, 5. - 6. Oktober 1989

/21/ Clausmeyer, H., K. Kussmaul und E. Roos: Der Einfluß des Spannungszustandes auf den Versagensablauf angerissener Bauteile aus Stahl. Mat.-wiss. u. Werkstofftechn. 20, 1989, pp. 101-117

/22/ Kußmaul, K., Clausmeyer, H., Roos, E. und Eisele U.: Definition eines Instabilitätskriteriums für überelastisch beanspruchte angerissene Bauteile. 20. MPA-Seminar, MPA Stuttgart, 6. - 7. Oktober 1994

/23/ Clausmeyer, H.:Über die Beanspruchung von Stahl bei mehrachsigen Spannungszuständen. Konstruktion 20, Heft 10, S. 395-401, 1968

/24/ Forschungsvorhaben RDB-Notkühlsimulation. Förderkennzeichen BMFT 150 0618, MPA Stuttgart, Abschlußbericht 1990

/25/ Forschungsvorhaben "Experimentelle und numerische Untersuchungen zum Verhalten eines niedrigzähen Behälterwerkstoffs bei Rißeinleitung, instabiler Rißausbreitung und Rißstopp bei überlagerten mechanischen und thermischen Beanspruchungen". BMFT-FKZ 150 0787, 1992

/26/ Forschungsvorhaben „Untersuchungen zu den Auswirkungen von Niederdrucktransienten bei simulierten Werkstoffzuständen". BMBF-FKZ 1500 946, 1996 (in print).

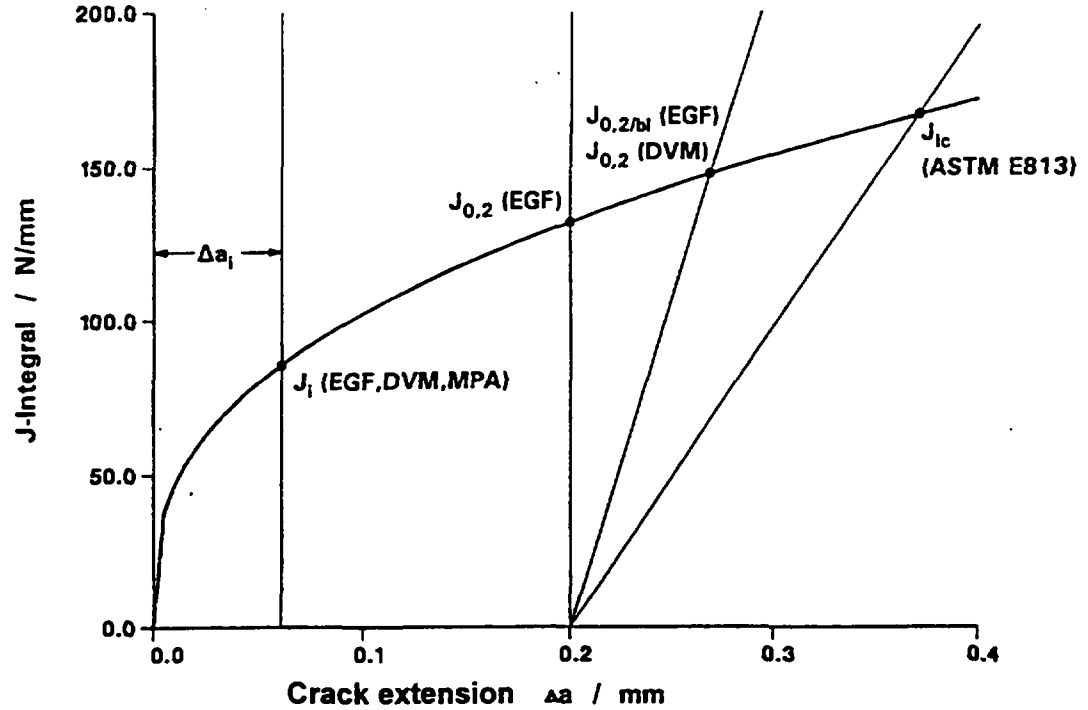

Fig. 1: Comparison of crack initiation values and pseudo initiation parameters according to different test standards

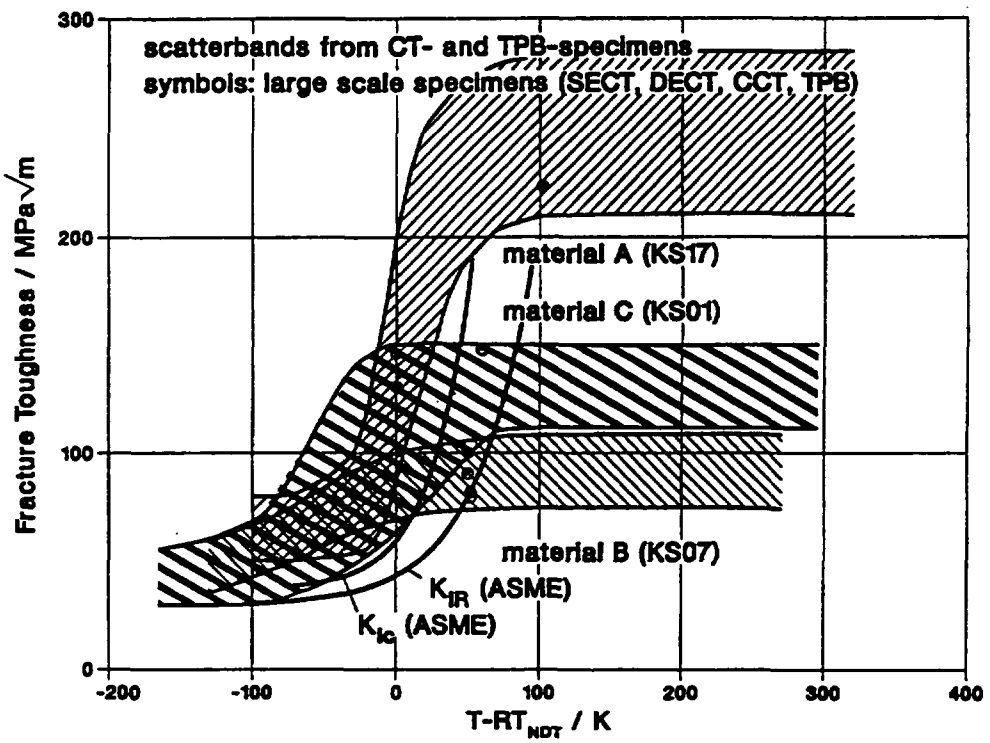

Fig. 2: Crack initiation values determined with large scale specimens in comparison with the scatter band derived from small scale specimen testing

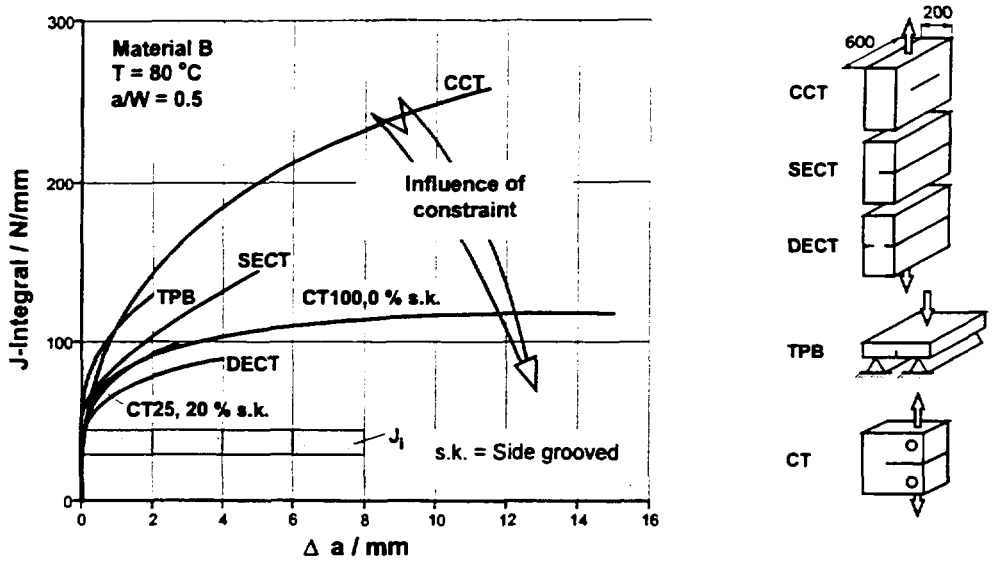

Fig. 3: Crack resistance curves of large scale specimens of different geometry with fatigue crack

Specimen	NKS4	NKS6	NT3
	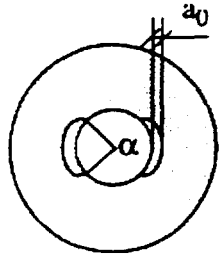	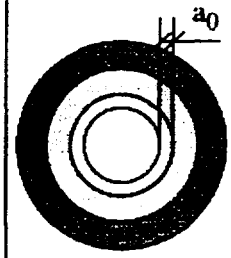	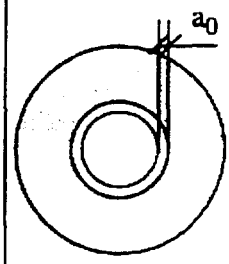
Material	22 NiMoCr 3 7	17 MoV 8 4 S3 NiMo 1	17 MoV 8 4
Dimensions	R_i = 200 mm R_a = 400 mm	R_i = 202 mm R_{Mat} = 296 mm R_a = 398 mm	R_i = 200 mm R_a = 395 mm
Geometry of crack	Circum. crack α = 52°	Circum. crack α = 360°	Circum. crack α = 360°
Crack depth	a_0 = 31,2/29,5mm a_0/W = 0,15	a_0 = 34 mm a_0/W = 0,17	a_0 = 20 mm a_0/W = 0,1

Fig. 4: Selected MPA thermal shock experiments

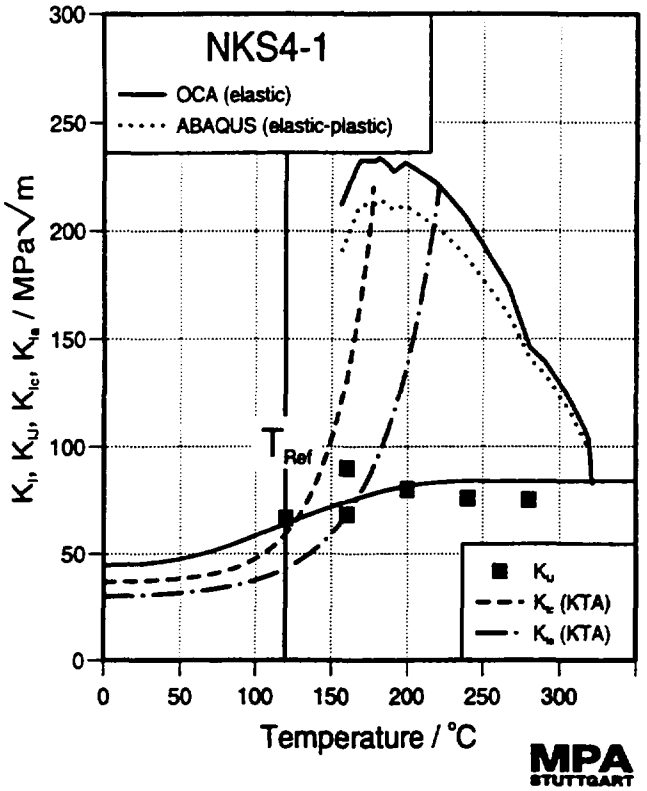

Fig. 5: Load path and fracture mechanics material parameters of thermal shock experiment NKS 4-1

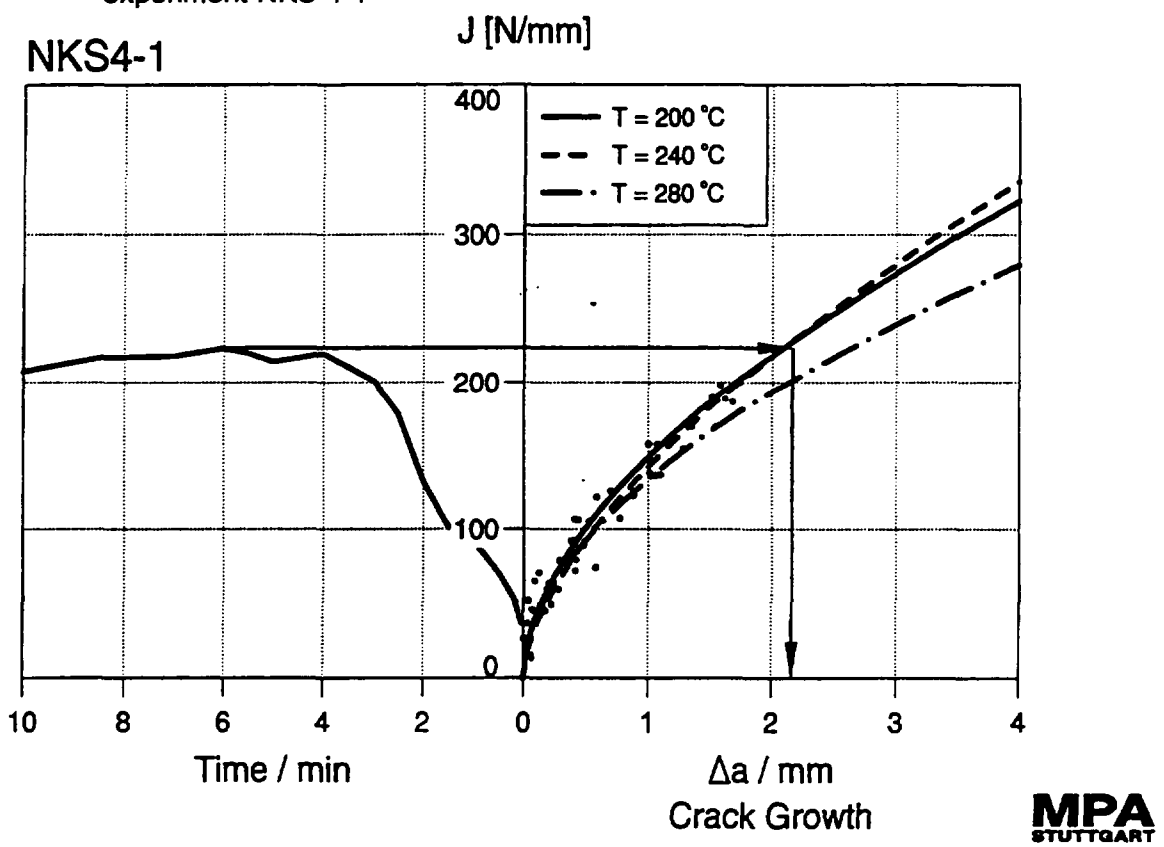

Fig. 6: Procedure to evaluate amount of stable crack extension from load path and crack resistance curve of thermal shock experiment NKS 4-1

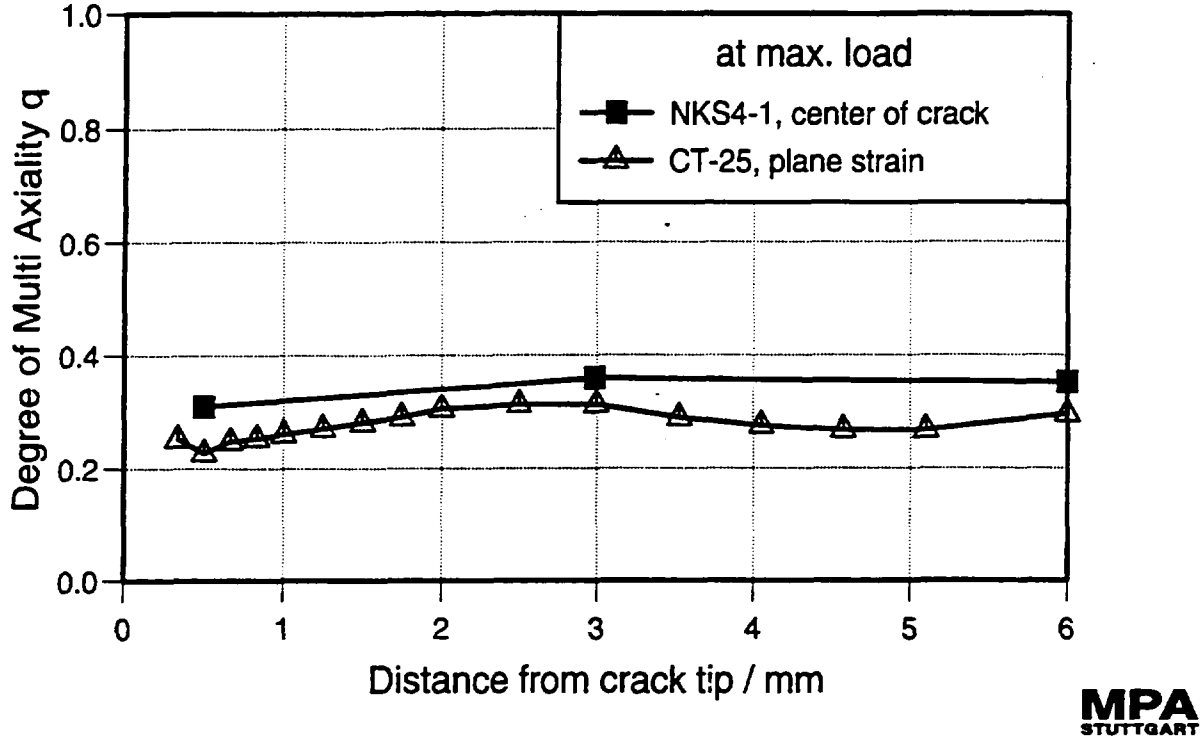

Fig. 7: Degree of multi-axiality q ahead of the crack tip of the thermal shock specimen NKS 4-1

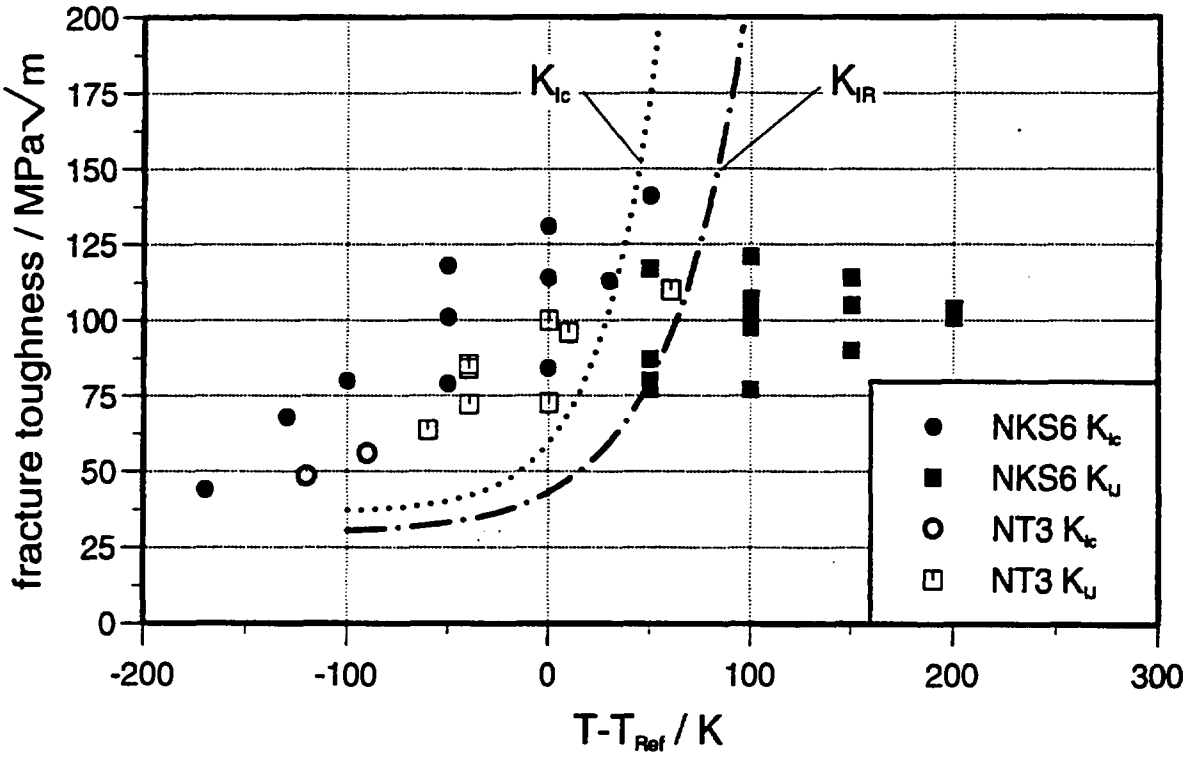

Fig. 8: Fracture toughness data K_{Ic} and K_{IJ} normalised to the transition temperature T_{ref} of the MoV steel of the thermal shock specimens NKS 6 and NT 3

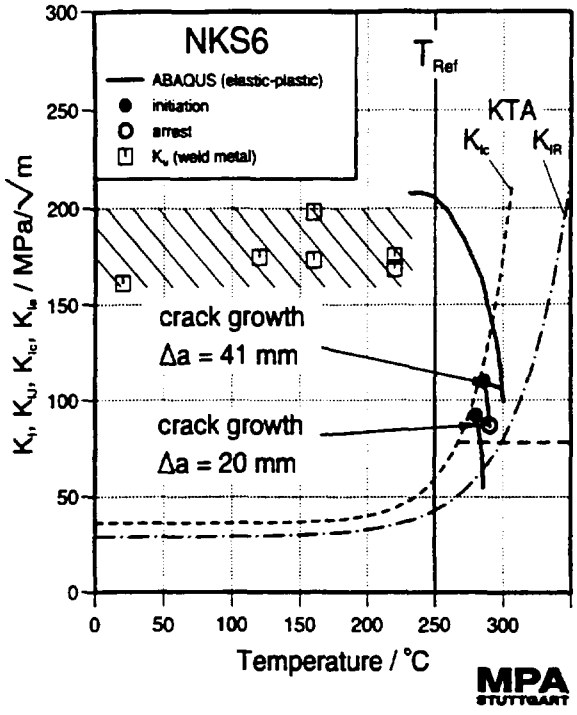

Fig. 9: Load path and fracture mechanics material parameters of thermal shock experiment NKS 6

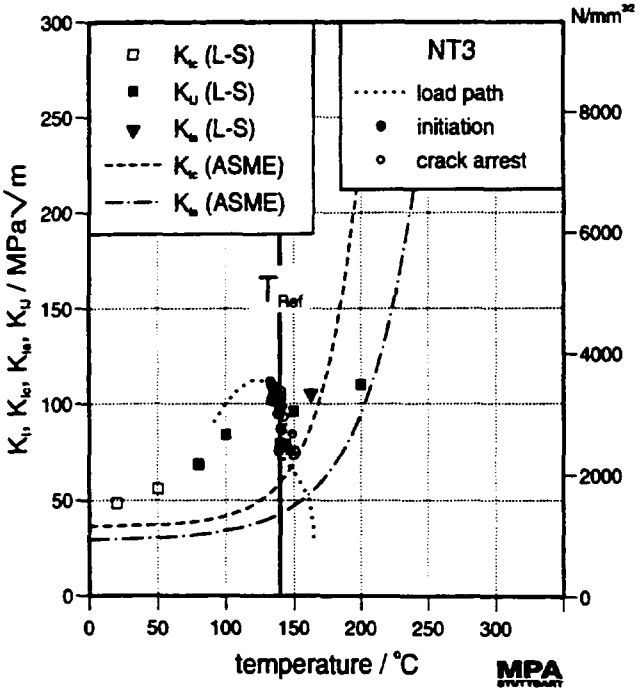

Fig. 10: Load path and fracture mechanics material parameters of thermal shock experiment NT 3

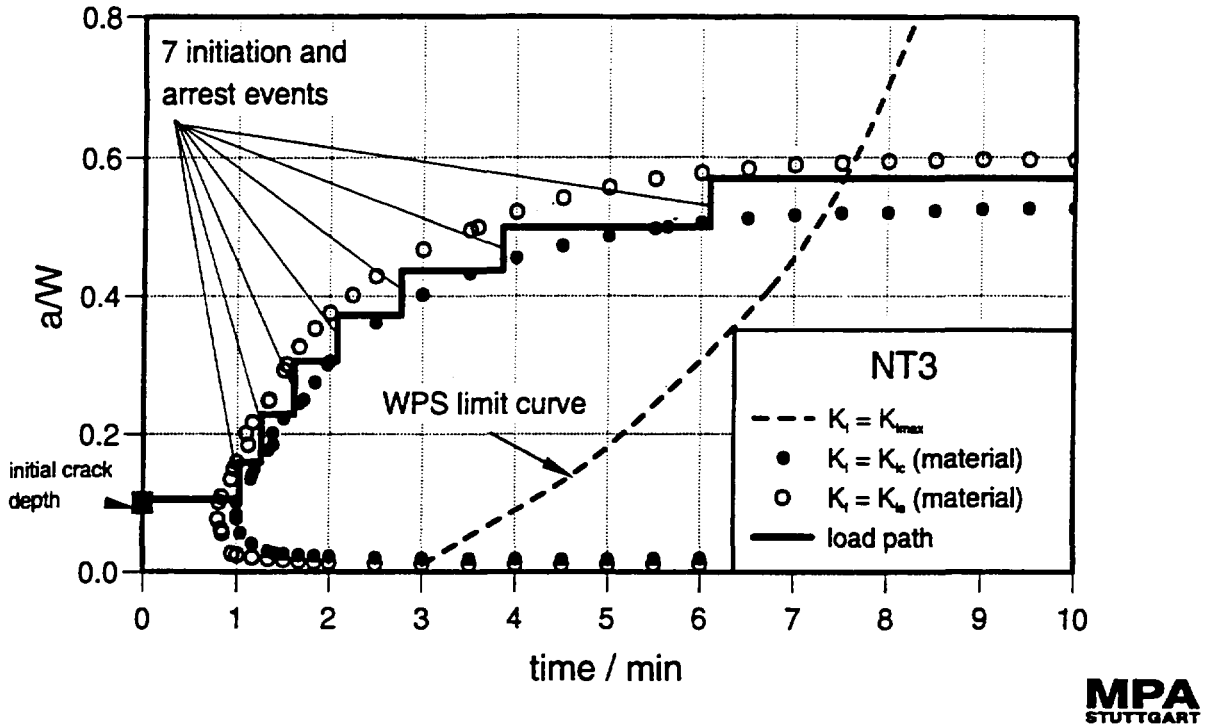

Fig. 11: Critical crack depth diagram of thermal shock experiment NT 3

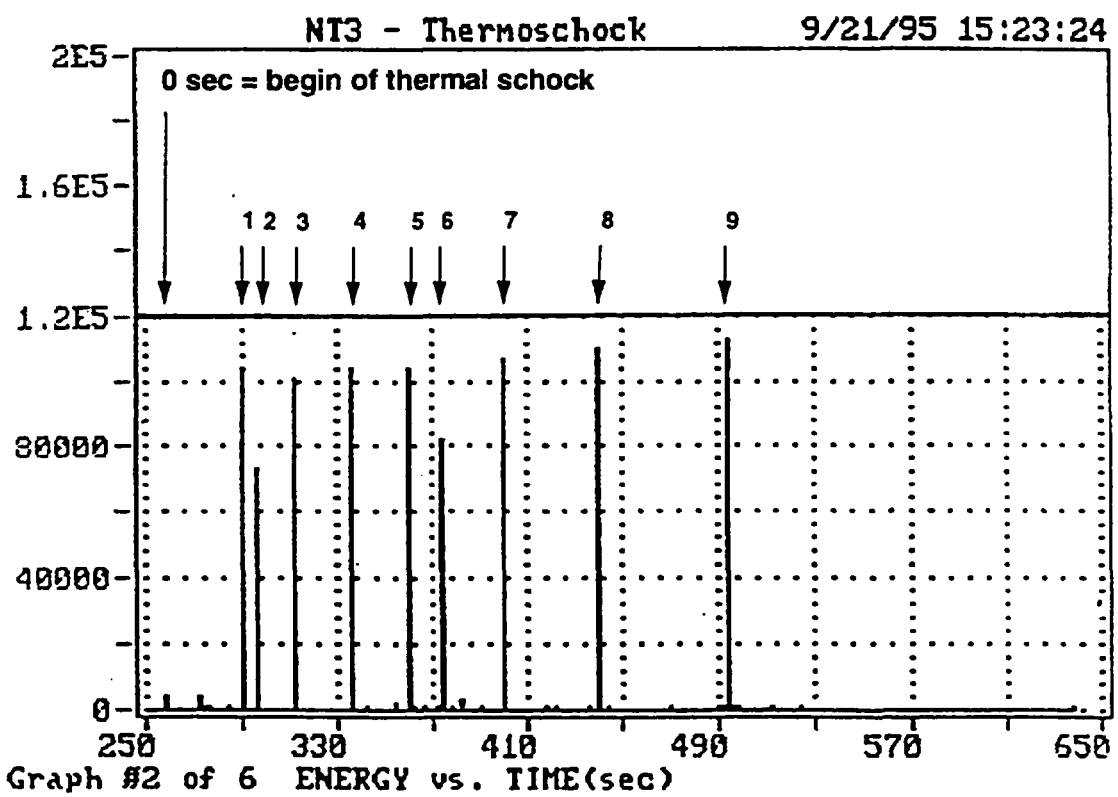

Fig. 12: Acoustic emission signals during thermal shock experiment NT 3